An Adaptive Algorithm based on $L_q\left(q=\frac{1}{2},1,2\right)$ Regularization for Image Restoration

QIANSHUN CHANG

School of Mathematics and Statistics, Jiangsu Normal University, Xuzhou 221116, China and Institute of Applied Mathematics, Academy of Mathematics and Systems Scientific, Chinese academy of Sciences, Beijing,
qschang@amss.ac.cn

Joint with Zengyan Che

I. Introduction

ROF model :

$$\arg\min_u ||\nabla u||_1 + \frac{\mu}{2}\|Ku - z\|_2^2 . \tag{1}$$

Minimization problem of L_q norm ,

$$\arg\min_u ||\nabla u||_q^q + \frac{\mu}{2}\|Ku - z\|_2^2 . \tag{2}$$

$q = 2$; $1 < q < 2$;

$q < 1$: non-convex,
$q = \frac{1}{2}$; $\frac{2}{3}$; $\frac{3}{4}$.

II. Basic Algorithms

anisotropic problem is considered :

$$\arg\min_{u} ||u_x||_q^q + ||u_y||_q^q + \frac{\mu}{2}\|Ku - z\|_2^2 . \tag{3}$$

Using the idea of the split Bregman method, the auxiliary variables

$$d_x \sim u_x, \qquad d_y \sim u_y.$$

$$(u^{k+1}, d^{k+1}) = \arg\min_{u,d_x,d_y} ||d_x||_q^q + ||d_y||_q^q + \frac{\mu}{2}\|Ku - z\|_2^2 + \frac{\lambda}{2}\|d_x - u_x\|_2^2$$

$$+\frac{\lambda}{2}\|d_y - u_y\|_2^2 , \tag{4}$$

where the last two items are added.

The minimization problem (4) is performed by iteratively minimizing with respect to u and d, separately. This yields the following three subproblems:

$$u^{k+1} = \arg\min_u \frac{\mu}{2}\left\|Ku - z + c^k\right\|_2^2 + \frac{\lambda}{2}\left\|d_x - u_x - b_x^k\right\|_2^2 + \frac{\lambda}{2}\left\|d_y - u_y - b_y^k\right\|_2^2, \tag{5}$$

$$d_x^{k+1} = \arg\min_{d_x} \|d_x\|_q^q + \frac{\lambda}{2}\left\|d_x - u_x^{k+1} - b_x^k\right\|_2^2, \tag{6}$$

$$d_y^{k+1} = \arg\min_{d_y} \|d_y\|_q^q + \frac{\lambda}{2}\left\|d_y - u_y^{k+1} - b_y^k\right\|_2^2, \tag{7}$$

where

$$b_x^{k+1} = b_x^k + \delta_b(u_x^{k+1} - d_x^{k+1}), \quad b_y^{k+1} = b_y^k + \delta_b(u_y^{k+1} - d_y^{k+1}), \tag{8}$$

$$c^{k+1} = c^k + \delta_c(Ku^{k+1} - z), \tag{9}$$

$\mu > 0, \quad \lambda > 0, \qquad 0 < \delta_b \leq 1 \qquad$ and $\qquad 0 < \delta_c < 2.$

Here the three variables b_x, b_y and c are added in the subproblems in order to improve the algorithm.

The subproblem (5) is quadratic and differentiable in u.

The corresponding Euler-Lagrange equation:

$$(\mu K^T K - \lambda \Delta) u^{k+1} = \mu K^T (z - c^k) + \lambda \nabla_x^T (d_x^k - b_x^k) + \lambda \nabla_y^T (d_y^k - b_y^k), \quad (10)$$

where $\Delta = -\nabla_x^T \nabla_x - \nabla_y^T \nabla_y$.

The equation (10) is discretized by the difference method as follows

$$(\mu K^T K u^{k+1} - \lambda \Delta u^{k+1})_{ij} = F_{ij}^k, \quad (11)$$

where

$$\Delta u_{ij}^{k+1} = -(4u_{ij}^{k+1} - u_{i+1,j}^{k+1} - u_{i-1,j}^{k+1} - u_{i,j+1}^{k+1} - u_{i,j-1}^{k+1}), \quad (12)$$

$$F_{ij}^k = \mu (K^T (z - c^k))_{ij} + \lambda [(d_x^k - b_x^k)_{i-1,j}$$

$$-(d_x^k - b_x^k)_{ij} + (d_y^k - b_y^k)_{i,j-1} - (d_y^k - b_y^k)_{ij}], \quad (13)$$

$$1 \le i \le I, \quad 1 \le j \le J.$$

The problem (11) is a linear algebraic system of equations and can be solved efficiently by our multigrid method. The number of the operations is $O(N)$.

Given a fixed u, the problems (6) and (7) of finding the optimal d_x and d_y consist of 2N independent 1D problems of the form:

$$\omega^* = \arg\min_{\omega} |\omega|^q + \frac{\lambda}{2}(\omega - v)^2, \tag{14}$$

since each term is positive in the minimization problems (6) and (7).

In the formula (14), ω denotes d_x or d_y, and v represents $(u_x^{k+1} - b_x^k)$ or $(u_y^{k+1} - b_y^k)$.

Let the cost function in (14) be

$$FC(\omega) = |\omega|^q + \frac{\lambda}{2}(\omega - v)^2. \tag{15}$$

The problem (14) is considered in the following three different situations:

1. $q = 2$.
   This is simple, since the cost function is differentiable.

Setting the derivative of (15) with regard to ω to zero implies that the optimal value

$$\omega^* = \frac{\lambda v}{2 + \lambda}. \tag{16}$$

Therefore, replacing the v with $(u_x^{k+1} - b_x^k)$ or $(u_y^{k+1} - b_y^k)$, we get

$$\begin{cases} d_{x,i,j}^{k+1} = \frac{\lambda(u_{x,i,j}^{k+1} + b_{x,i,j}^k)}{2+\lambda}), \\ d_{y,i,j}^{k+1} = \frac{\lambda(u_{y,i,j}^{k+1} + b_{y,i,j}^k)}{2+\lambda}). \end{cases} \tag{17}$$

2. $q = 1$.

The problem (14) is solved by shrinkage operator and the optimal value is

$$\omega^* = shrink(v, \quad \frac{1}{\lambda}).$$

Hence,

$$\begin{cases} d_{x,i,j}^{k+1} = shrink(u_{x,i,j}^{k+1} + b_{x,i,j}^{k}, \quad \frac{1}{\lambda}), \\ d_{y,i,j}^{k+1} = shrink(u_{y,i,j}^{k+1} + b_{y,i,j}^{k}, \quad \frac{1}{\lambda}), \end{cases} \tag{18}$$

where

$$shrink(x, \gamma) = \frac{x}{|x|} \cdot \max(|x| - \gamma, 0). \tag{19}$$

The formula (18) is explicit.

3. $0 < q < 1$.

For general values of q , setting the derivative of the cost function (15) with regard to ω to zero gives a nonlinear algebraic equation,

$$q|\omega|^{q-1} sign(\omega) + \lambda(\omega - v) = 0. \tag{20}$$

which may be solved by Newton's iteration algorithm in general.

For some specific values of q, for example, $q = \frac{1}{2}$, $q = \frac{2}{3}$ and $q = \frac{3}{4}$, it is possible to derive an exact solution of the problem (14).

In this paper, $q = \frac{1}{2}$ is used, since it can be a representative for $0 < q < 1$.

With $q = \frac{1}{2}$, by transforming the (20) into identity and squaring both sides of the identity, we obtain

$$|\omega|^{-1} = 4\lambda^2(v - \omega)^2, \tag{21}$$

which is rewritten as

$$\omega^3 - 2v\omega^2 + v^2\omega - sign(\omega)/4\lambda^2 = 0. \tag{22}$$

According to the minimization problem (14) , ω^* must lie between 0 and v. Then we can replace $sign(\omega)$ with $sign(v)$ and have

$$\omega^3 - 2v\omega^2 + v^2\omega - sign(v)/4\lambda^2 = 0. \tag{23}$$

The three roots of the cubic algebraic equation (23) may be obtained by Cardano's formula. The rest problem is to determine which root corresponds to the global minima of (14).

There are three kinds of situations for the roots of cubic equation (23) :

(a) 3 imaginary roots : The lack of real roots means that the derivative of the cost function $FC(\omega)$ never is negative, thus $\omega^* = 0$.

(b) 2 imaginary roots and 1 real roots r : If $FC(r) < FC(0)$, then $\omega^* = r$. Otherwise, $\omega^* = 0$.

(c) 3 real roots : Examing (21) and (22), the reduction introduces a spurious root out of the interval [0, v]. This root should be ignored because ω^* must lie between 0 and v.

Hence, we need to choose a value in other two real roots and 0 as ω^* such the cost function (15) is the smallest.

Algorithm for solving the minimization problem (14) for $q = \frac{1}{2}$:

Given: value v, Weight λ,

1.Compute intermediary terms m, t_1, t_2, t_3 :

$m = -sign(v)/4\lambda^2$

$t_1 = 2v/3$

$t_2 = \sqrt[3]{-27m - 2v^3 + 3\sqrt{3}\sqrt{27m^2 + 4mv^3}})$

$t_3 = v^2/t_2$

2. Compute 3 roots r_1, r_2, r_3 :

$r_1 = t_1 + 1/(3 \cdot 2^{1/3}) \cdot t_2 + 2^{1/3}/3 \cdot t_3$

$r_2 = t_1 - (1 - \sqrt{3}i)/(6 \cdot 2^{1/3}) \cdot t_2 - (1 + \sqrt{3}i)/(3 \cdot 2^{2/3}) \cdot t_3$

$r_3 = t_1 - (1 + \sqrt{3}i)/(6 \cdot 2^{1/3}) \cdot t_2 - (1 - \sqrt{3}i)/(3 \cdot 2^{2/3}) \cdot t_3$

3. Pick global minimum from $(0, r_1, r_2, r_3)$

Choose a value in $(0, r_1, r_2, r_3)$ as ω^* such that such the cost function is the smallest and the ω^* is in the interval [0, v].

return ω^*

III Our Adaptive Algorithm Our adaptive algorithm is the combination of three algorithms .

Thus, we apply the following continuous linear formula to assemble the three algorihtms with different norms :

$$\begin{cases} L_2, & if \quad |\nabla u| \le C_0, \\ V_1 + \frac{|\nabla u| - C_0}{C_1 - C_0}(V_1 - V_2), & if \quad C_0 < |\nabla u| \le C_1, \\ L_1, & if \quad C_1 < |\nabla u| \le C_2, \\ V_1 + \frac{|\nabla u| - C_2}{C_3 - C_2}(V_{\frac{1}{2}} - V_1), & if \quad C_2 < |\nabla u| \le C_3, \\ L_{\frac{1}{2}}, & if \quad |\nabla u| \ge C_3. \end{cases} \tag{24}$$

where $V_i (i = 1, 2, \frac{1}{2})$ denote the solutions of the algorithms for the $L_i (i = 1, 2, \frac{1}{2})$ norm, respectively, and $C_i (i = 0, 1, 2, 3)$ are constants.

In computation, The parameters $C_i (i = 0, 1, 2, 3)$ are taken as 5, 8, 15, 20, respectively, for the most images and are properly modified for some images.

This adaptive algorithm can avoid artificial discontinuity in the image restoration.

The algorithm for L_2 norm is used in the flat regions, where the values of $|\nabla u|$ is small.

The algorithm for $L_{\frac{1}{2}}$ norm is applied in the jumps, where the values of $|\nabla u|$ is large.

When the values of $|\nabla u|$ is moderate, the algorithm for L_1 norm is used.

IV Numerical Experiments

The six original images are shown in Fig.1.

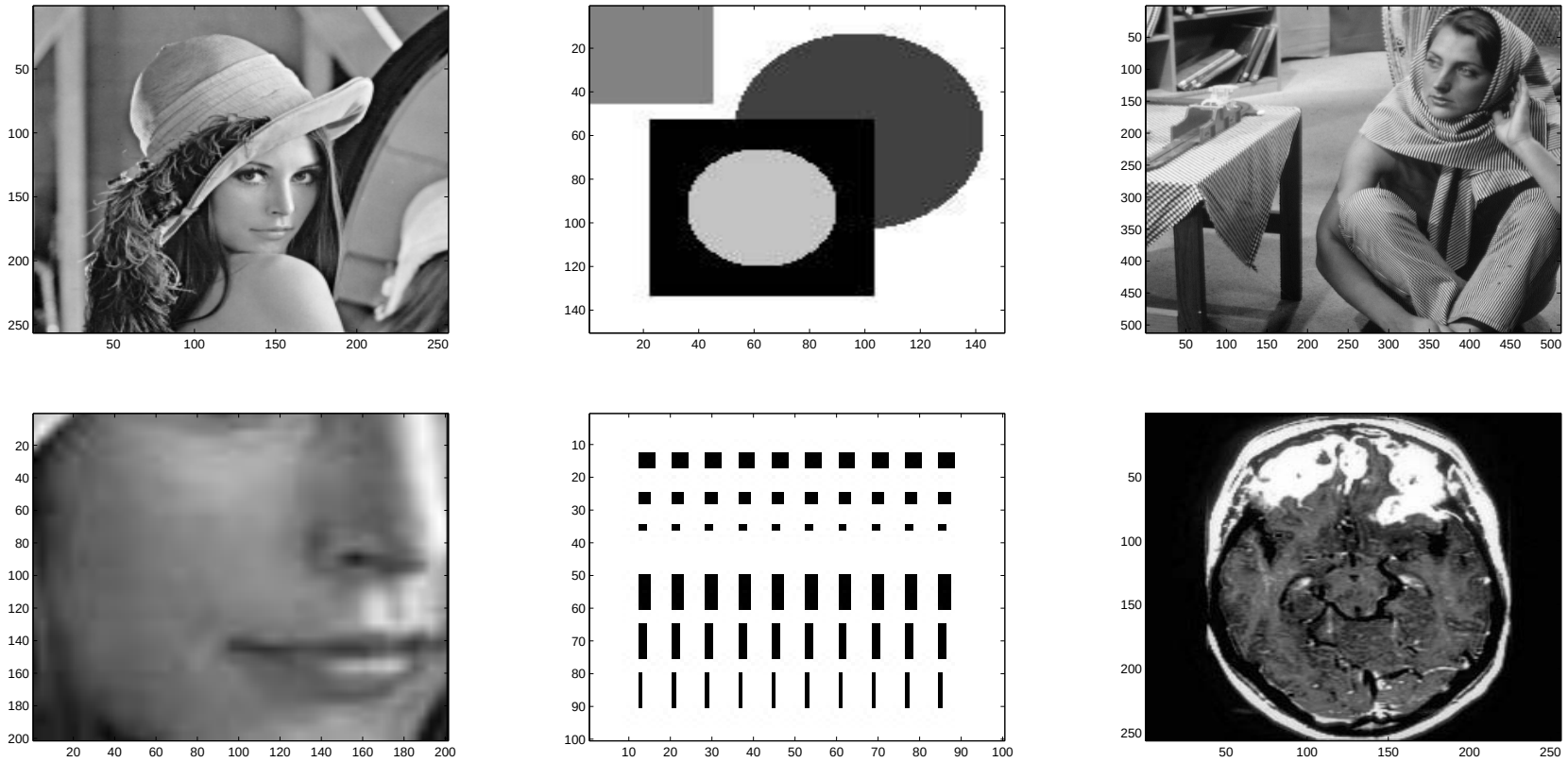

Fig. 1 Original images. Top: Lena 256*256 (left); Shape 150*150 (middle); Barbara 512*512(right) ; Bottom: Lena-face 201*201 (left); tv-fig5 100*100 (middle); MRI 256*256 (right)

The five combination algorithms:

SB : split Bregman method ;

AD : combination with three norms L_1, L_2 and $L_{\frac{1}{2}}$;

NAI : combination with L_1 norm and L_2 ;

NAII : combination with L_1 norm and $L_{\frac{1}{2}}$ norm ;

NAIII : combination with $L_{1/2}$ norm and L_2 norm .

Exam. 1 Lena image degraded by the blur " out of focus with radius 4 " and a noise.

Table 1. Results for the "Lena" image.

σ	Al.	PARA.	N	PSNR
10	SB	1.5, 0.25	5	22.37
	AD		4	22.57
	NAI		3	22.42
	NAII		3	22.49
	NAIII		4	22.35
20	SB	0.4, 0.25	5	21.40
	AD		4	21.56
	NAI		5	21.48
	NAII		4	21.53
	NAIII		5	21.26
30	SB	0.25, 0.25	6	20.64
	AD		4	20.85
	NAI		4	20.77
	NAII		4	20.80
	NAIII		5	20.61

Exam. 2 The "Shape" image degraded by a scattering blur $(1, 2, 3, 16, 3, 2,$ $(1, 2, 3, 16, 3, 2, 1)/784$.

Table 2. Results for the "Shape" image.

σ	Al.	PARA.	N	PSNR
5	SB	2.5, 0.25	6	27.91
	AD		7	28.80
	NAI		6	28.96
	NAII		6	27.65
	NAIII		7	29.85
10	SB	1.0, 0.25	5	24.65
	AD		5	24.82
	NAI		4	24.57
	NAII		5	24.51
	NAIII		5	25.34
20	SB	0.4, 0.25	5	21.88
	AD		5	22.00
	NAI		5	22.17
	NAII		5	21.76
	NAIII		5	22.41

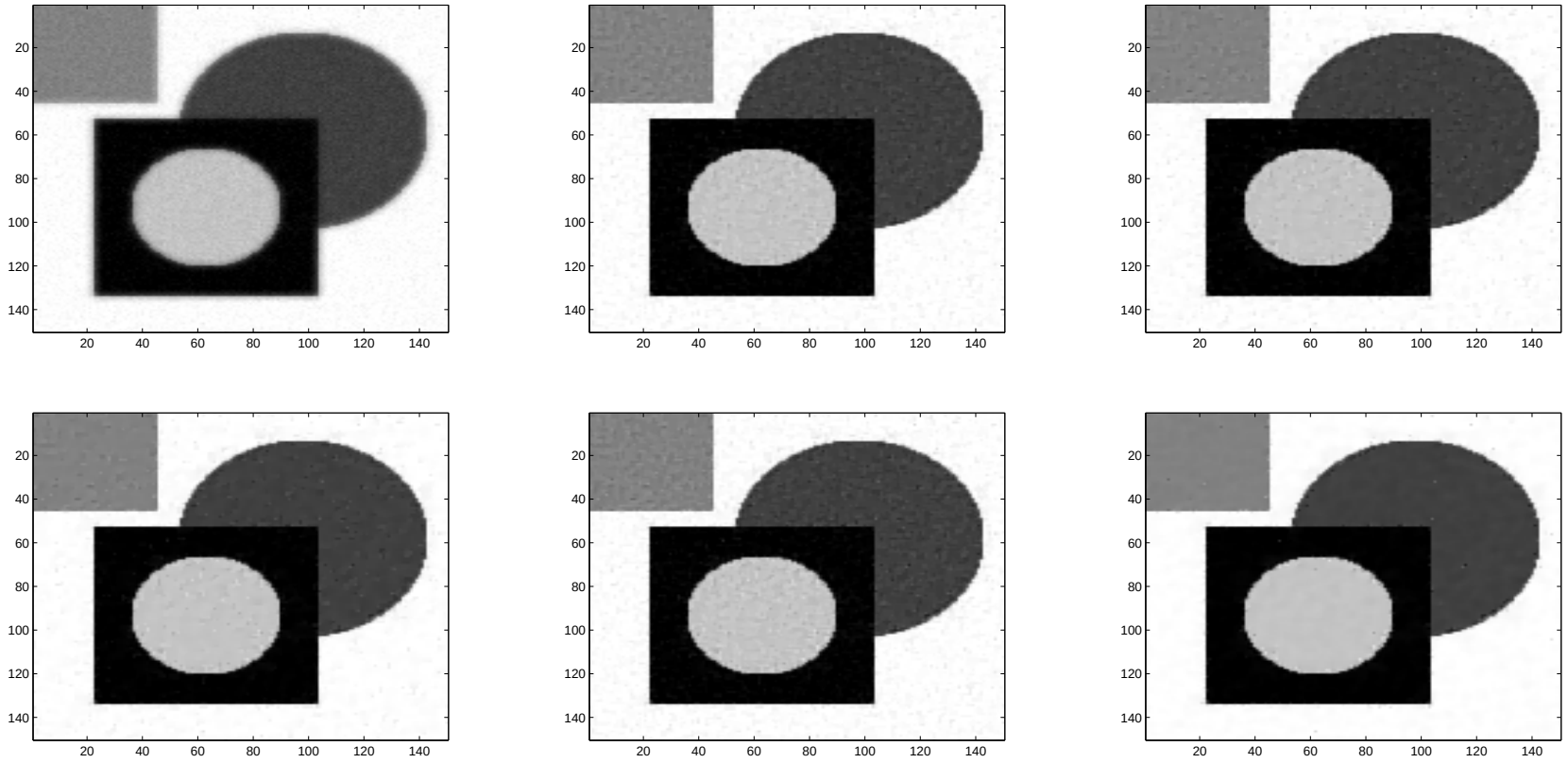

Fig. 2 Comparison of different algorithms for Exam. 2. Top : Noisy and blurred image (left), restored image by SB (middle) and restored image by AD (right) ; bottom : restored image by NAI (left), restored image by NAII (middle) and restored image by NAIII (right) for Shape image 150*150, σ=5 and scattering blur.

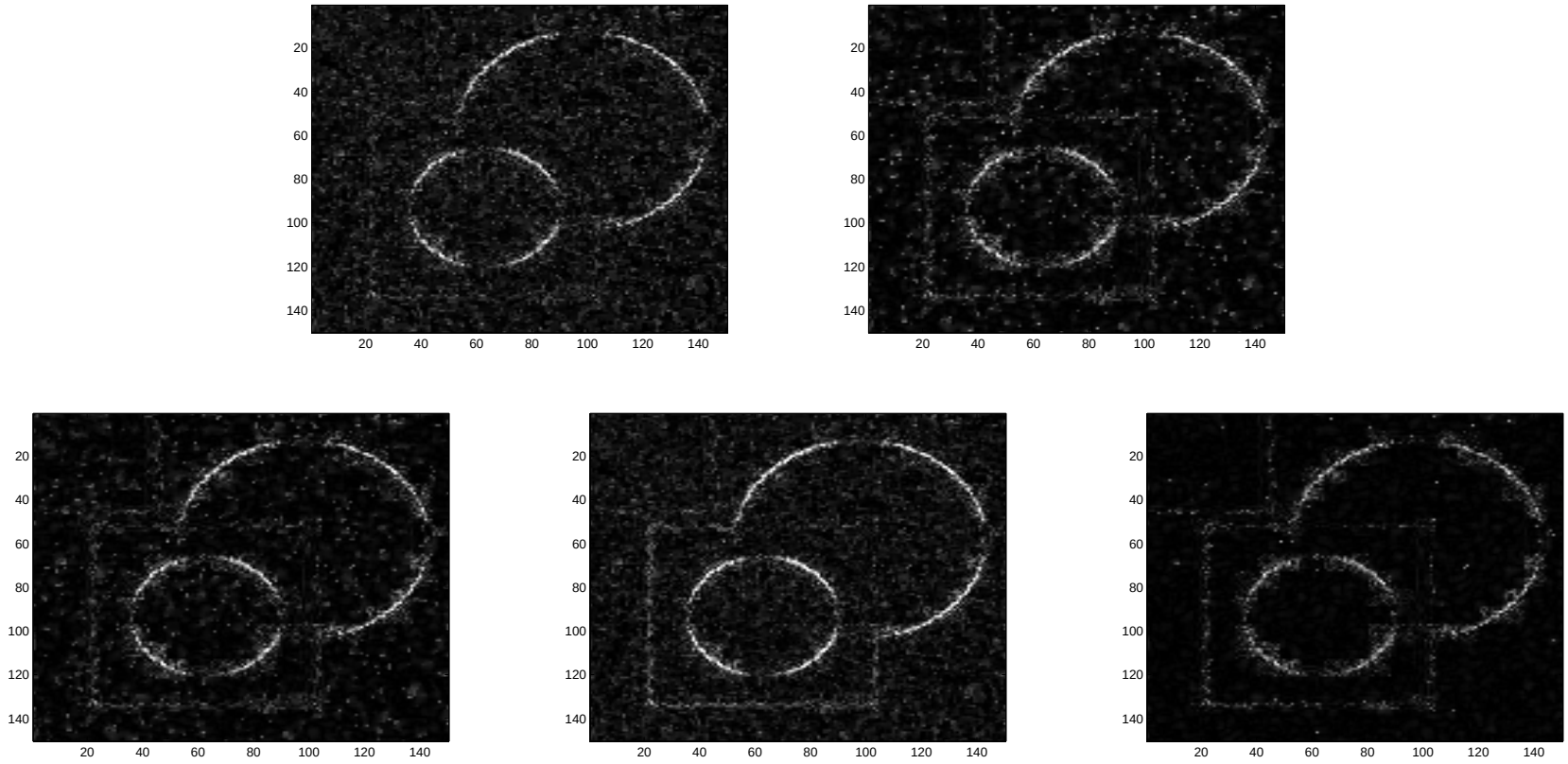

Fig. 3 Comparison of the images difference $z0 - u$ for different algorithms. Top : difference image of SB (left), difference image of AD (middle) ; bottom : difference image of NAI (left), difference image of NAII (middle) and difference image of NAIII (right) for Shape image 150*150, σ=5 and scattering blur .

Exam. 3 Barbara image degraded only degraded with a noise of the standard deviation σ.

Table 3. Computational results of Barbara image.

σ	Al.	PARA.	N	PSNR
5	SB	1.1, 0.25	5	29.78
	AD		4	30.07
	NAI		4	29.85
	NAII		4	29.95
	NAIII		4	30.12
10	SB	0.45, 0.25	6	24.87
	AD		5	25.15
	NAI		5	24.95
	NAII		5	25.02
	NAIII		5	25.23
20	SB	0.2, 0.25	5	20.59
	AD		5	20.72
	NAI		5	20.68
	NAII		5	20.64
	NAIII		5	20.78

Exam. 4 The Lena-face image just degraded by a noise with the standard deviation σ

Table 4. Computational results of Lena-face image with noise

σ	Al.	PARA.	N	PSNR
10	SB	0.5, 0.25	3	28.72
	AD		3	31.06
	NAI		3	31.05
	NAII		3	27.86
	NAIII		3	31.10
20	SB	0.2, 0.25	4	25.31
	AD		4	28.35
	NAI		4	28.24
	NAII		4	24.25
	NAIII		4	28.30
30	SB	0.16, 0.25	5	22.81
	AD		5	26.51
	NAI		5	26.47
	NAII		5	22.30
	NAIII		5	26.54

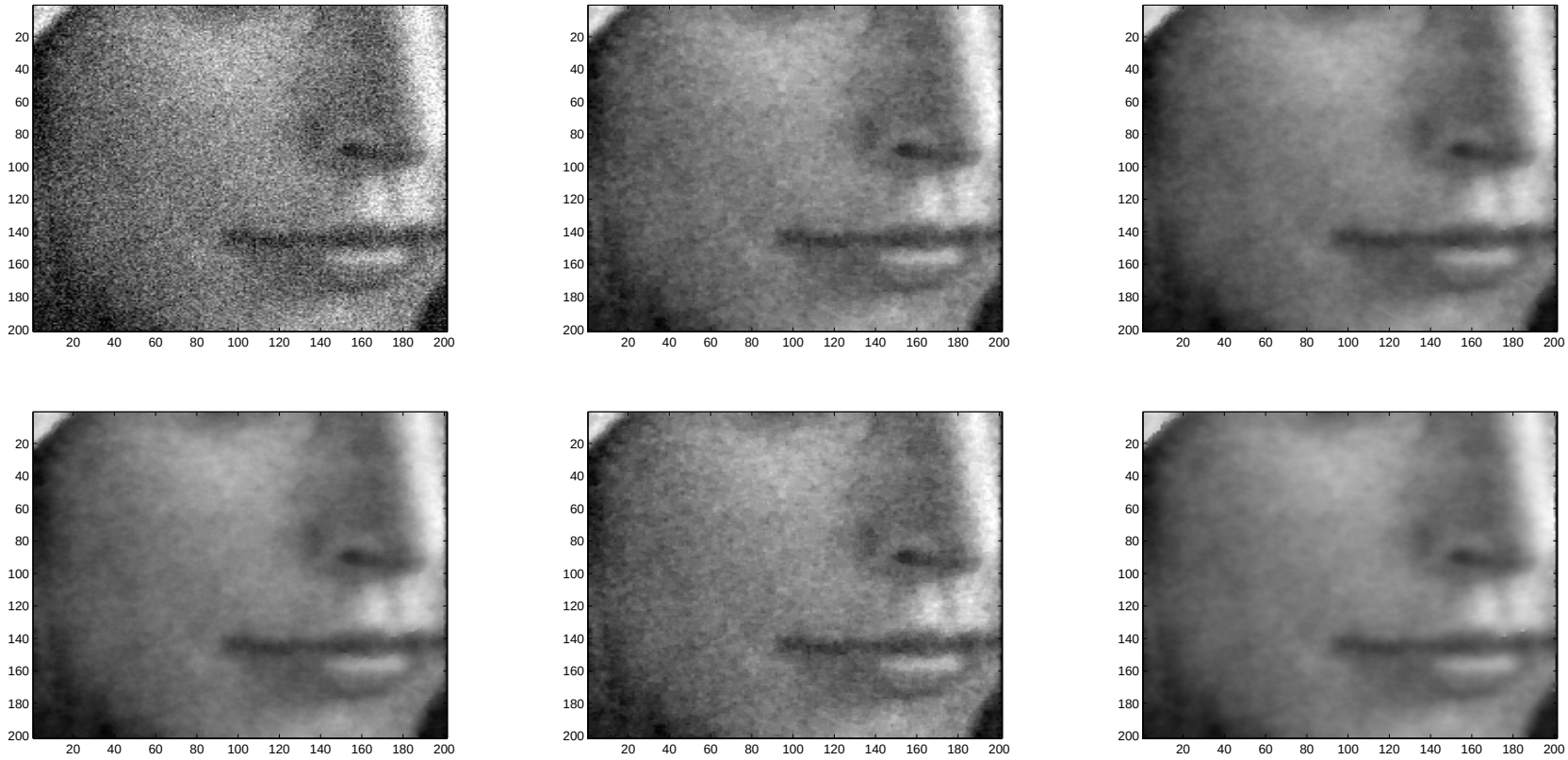

Fig.4 Comparison of different algorithms for Exam. 4. Top : Noisy and blurred image (left), restored image by SB (middle) and restored image by AD (right) ; bottom : restored image by NAI (left), restored image by NAII (middle) and restored image by NAIII (right) for Lena-face image 201*201, σ=30.

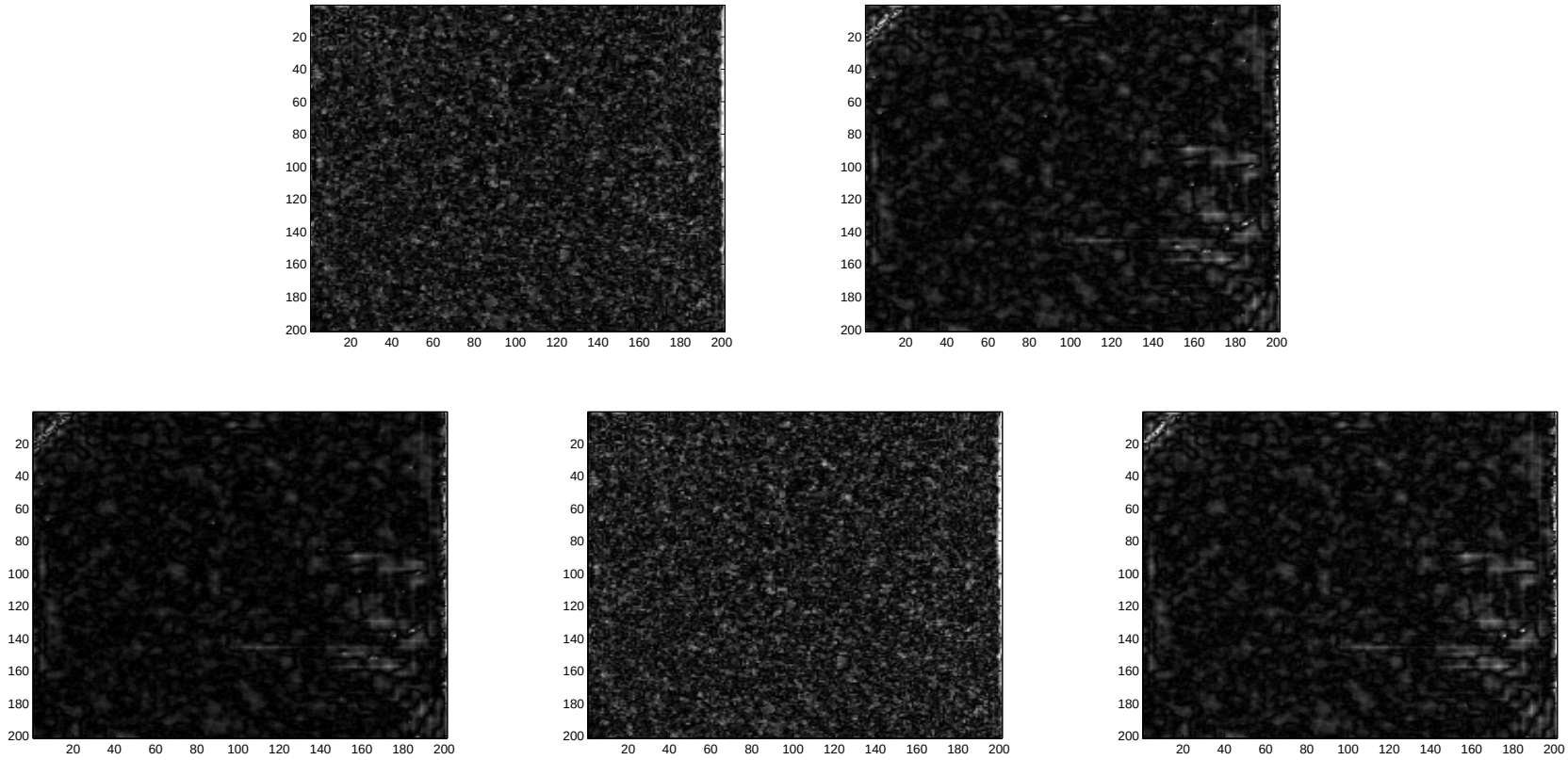

Fig. 5 Comparison of the images difference $z0 - u$ for different algorithms. Top : difference image of SB (left), difference image of AD (middle) ; bottom : difference image of NAI (left), difference image of NAII (middle) and difference image of NAIII (right) for Lena-face image 201*201, σ=30.

Exam. 5 he tv-fig5 image just degraded by a noise with the standard deviation σ.

Table 5. Computational results of the tv-fig5 image.

σ	Al.	PARA.	N	PSNR
10	SB	0.45, 0.25	7	31.53
	AD		8	38.99
	NAI		6	35.01
	NAII		6	31.47
	NAIII		8	39.27
20	SB	0.3, 0.25	8	25.21
	AD		7	29.61
	NAI		7	29.73
	NAII		6	24.91
	NAIII		7	32.14
30	SB	0.1, 0.25	13	20.91
	AD		9	24.44
	NAI		13	25.92
	NAII		9	20.29
	NAIII		11	27.78

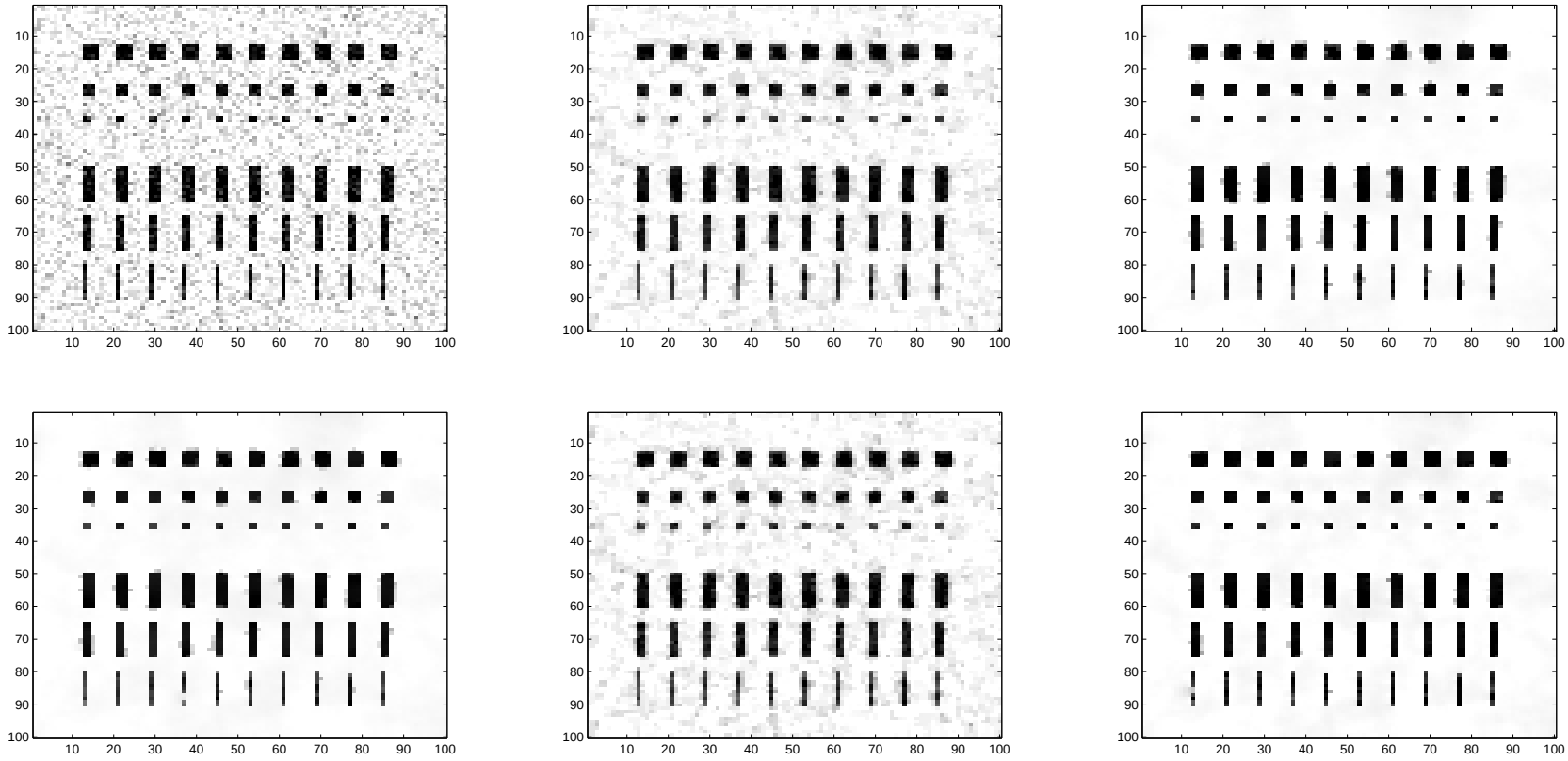

Fig. 6 Comparison of different algorithms for Exam. 5. Top : Noisy and blurred image (left), restored image by SB (middle) and restored image by AD (right) ; bottom : restored image by NAI (left), restored image by NAII (middle) and restored image by NAIII (right) for tv-fig5 image 100*100, σ=40.

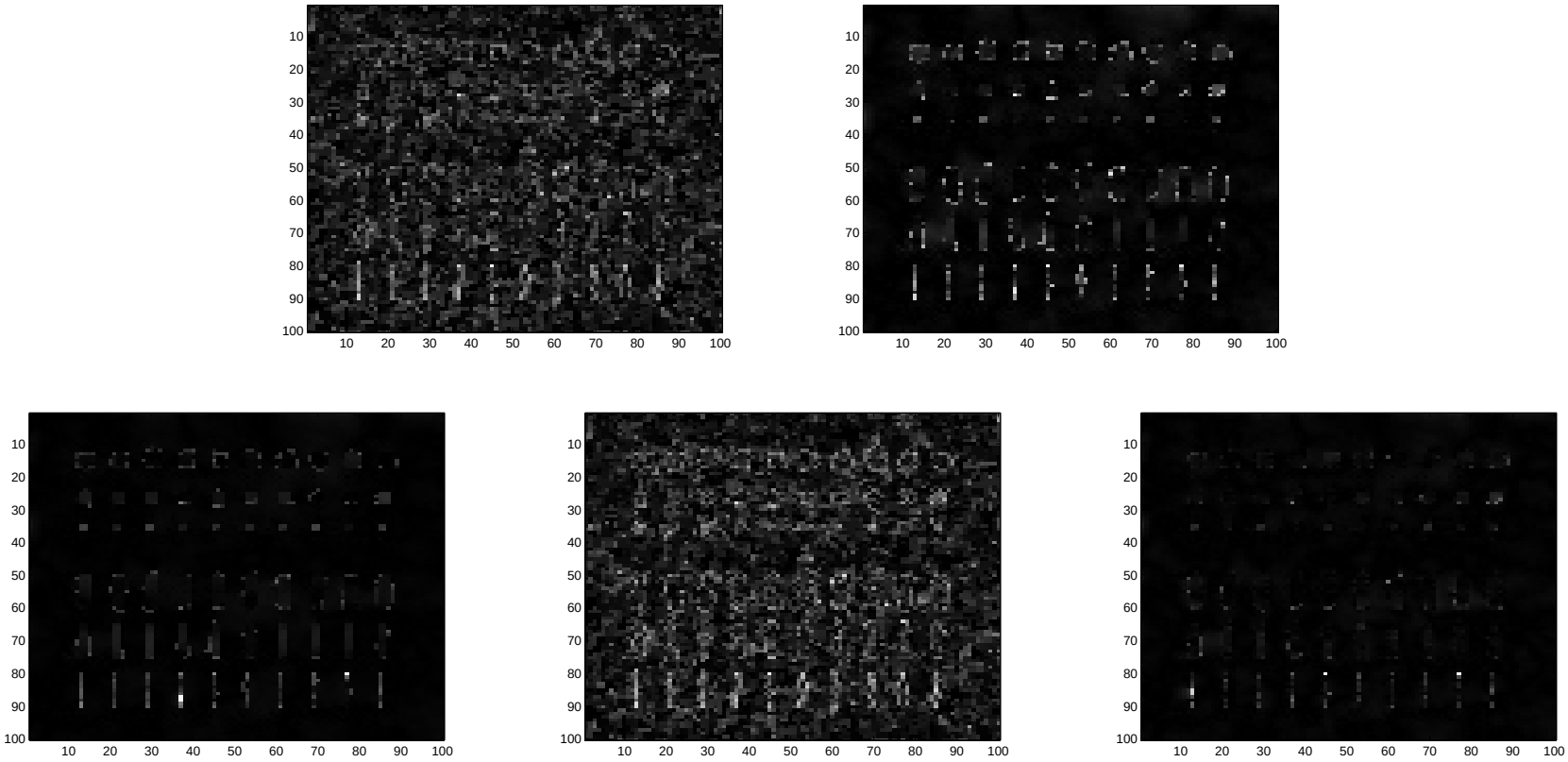

Fig. 7 Comparison of the images difference $z0 - u$ for different algorithms. Top : difference image of SB (left), difference image of AD (middle) ; bottom : difference image of NAI (left), difference image of NAII (middle) and difference image of NAIII (right) for tv-fig5 image 100*100, σ=40.

Exam. 6 An MRI image just degraded by a noise with the standard deviation σ.

Table 6. Computational results of an MRI image.

σ	Al.	PARA.	N	PSNR
5	SB	1.2, 0.25	4	28.25
	AD		3	28.82
	NAI		3	28.80
	NAII		3	28.46
	NAIII		3	28.70
10	SB	0.6, 0.25	5	23.70
	AD		5	24.50
	NAI		5	24.43
	NAII		5	23.78
	NAIII		5	24.34
15	SB	0.4, 0.25	4	20.75
	AD		3	21.79
	NAI		3	21.74
	NAII		3	21.21
	NAIII		3	21.40

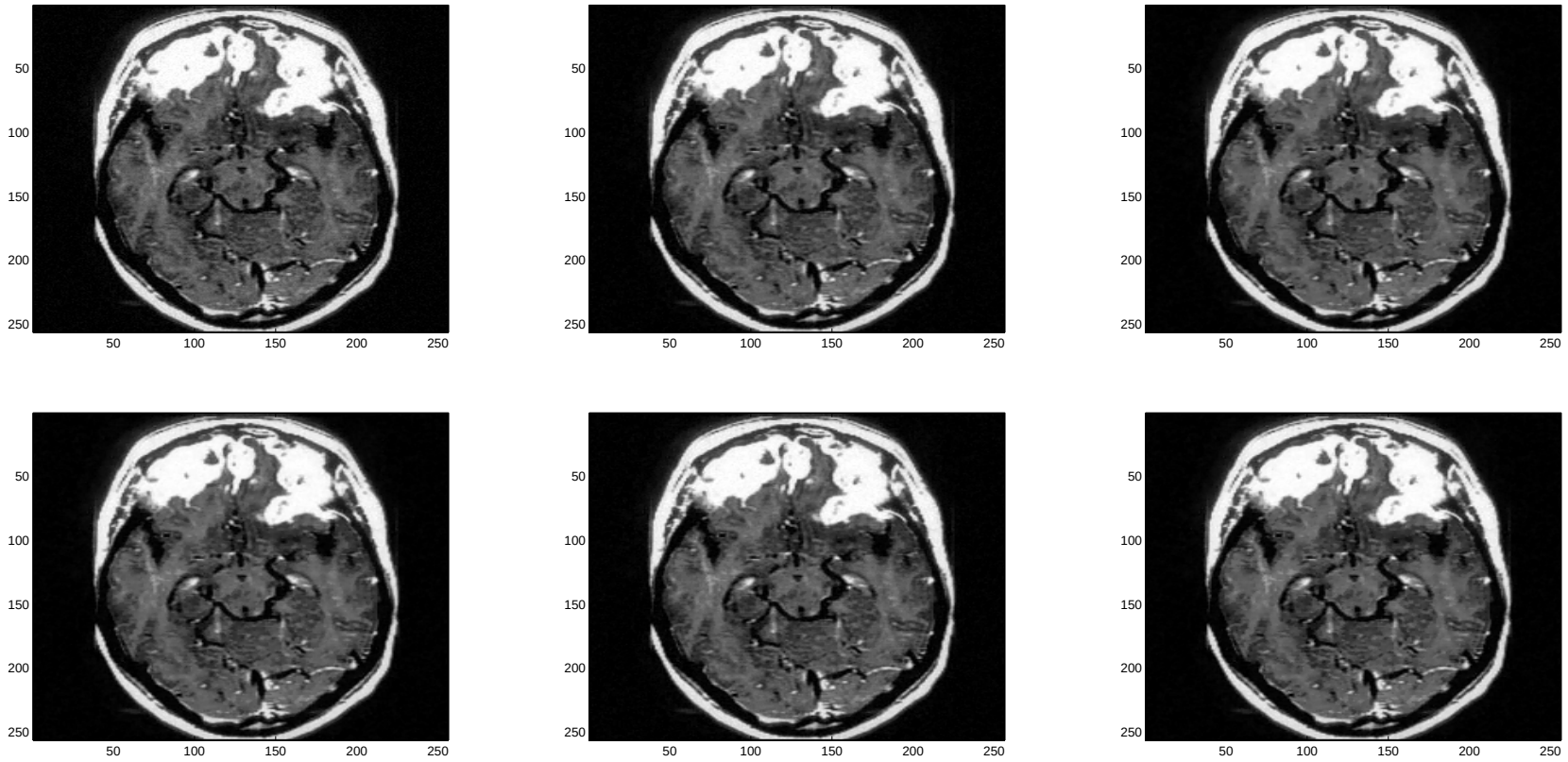

Fig. 8 Comparison of different algorithms for Exam. 6. Top : Noisy and blurred image (left), restored image by SB (middle) and restored image by AD (right) ; bottom : restored image by NAI (left), restored image by NAII (middle) and restored image by NAIII (right) for MRI image 256*256, σ=5.

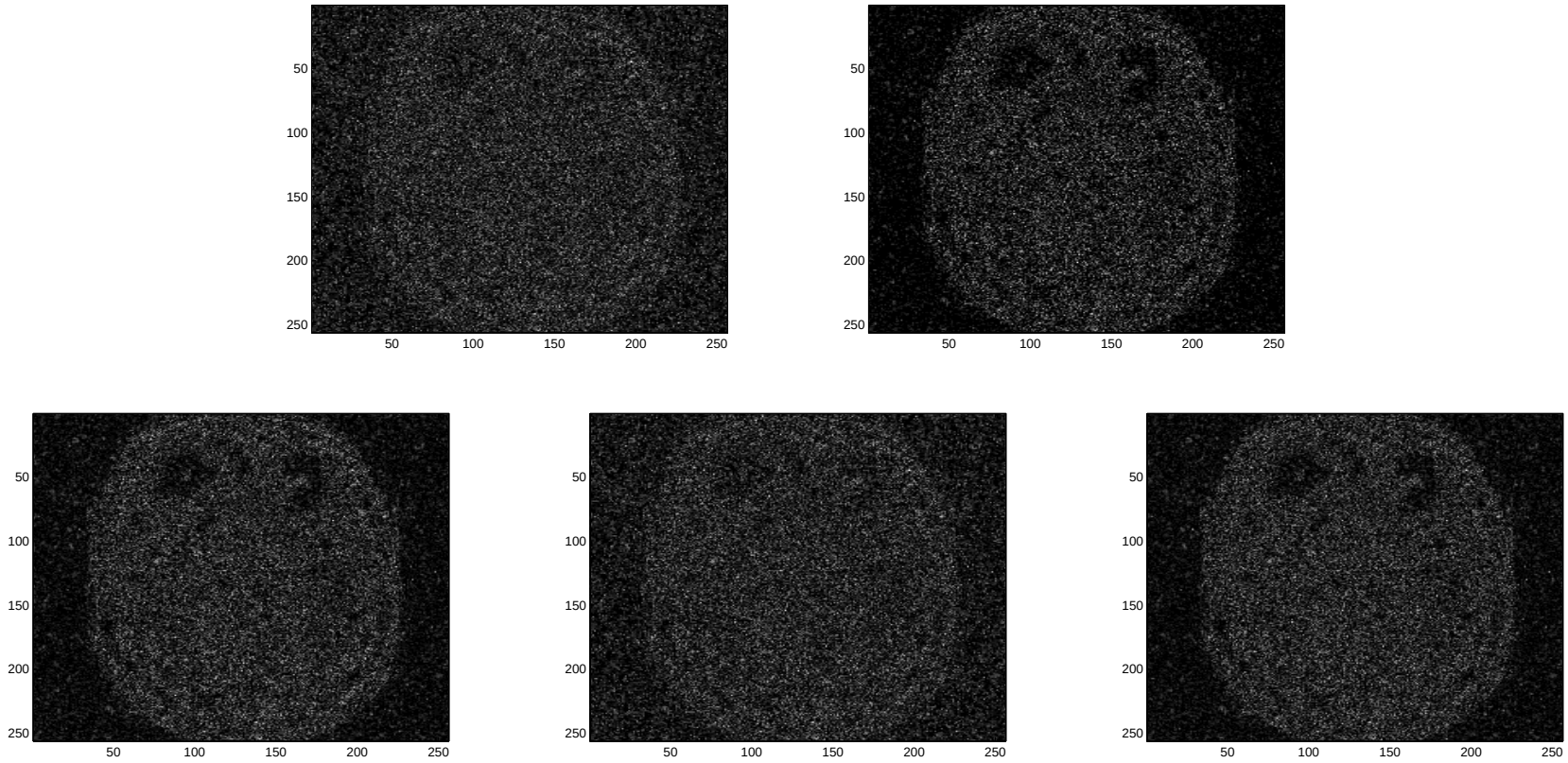

Fig. 9 Comparison of the images difference $z0 - u$ for different algorithms. Top : difference image of SB (left), difference image of AD (middle) ; bottom : difference image of NAI (left), difference image of NAII (middle) and difference image of NAIII (right) for MRI image 256*256, σ=5.

V Conclusion

In this paper, we propose an adaptive algorithm for the TV-based model of three norms $L_q\left(q=\frac{1}{2},1,2\right)$ for the image restoration problem.

We have the following conclusions from the results of numerical experiments:

1. The adaptive algorithms of using combination of norms $L_q\left(q=\frac{1}{2},1,2\right)$ can be applied for the image restoration and obtain satisfactory results for many images.

2. It is clear that the effect of algorithm of using different norms mainly lies in the removal of noise. Therefore, the adaptive algorithms of using combination of norms $L_q\left(q=\frac{1}{2},1,2\right)$ have better results than the SB algorithm (using the L_1 norm only) for the image denoising problem.

3. For the images with large smooth areas, for example, the Lena-face image, it is evident from Table 4, Image 4 and Image 5 that the algorithms NAI, NAIII and AD of using the L_2 norm are much better than SB and NAII.

Hence, the algorithm of using the L_2 norm should be combined in restoration methods for such images.

4. The "Shape" image and the "tv-fig5" image are composed of flat regions and boundary lines. We know form Example 2 and Example 5 that the algorithm NAIII of combining the L_2 norm $L_{1/2}$ is the best of the five algorithms, since the algorithm of using L_2 norm is suitable for the flat regions while the algorithm of using $L_{\frac{1}{2}}$ norm is suitable for the boundary lines.

5. For the real MRI image, the algorithm AD of using three norms is efficient. There are detailed constructions and complicated varieties in

many practical images. The combination algorithm AD selects different suitable algorithms for different areas.

Thus, the algorithm AD is useful for many practical images.

Therefore, the numerical results demonstrate that our adaptive algorithm can not only keep the original edge and original detailed information but also weaken the staircase phenomenon in the restored images.

The three algorithms are applied for different regions of a given image such that the advantages of each algorithm is adopted.

Therefore, our adaptive algorithm is efficient and robust even for images with large noises.

THANKS !